JOURNAL OF Materials CHEMISTRY

α-Sialon ceramics synthesised from a clay precursor by carbothermal reduction and nitridation

Thommy Ekström,*[a] Zhijian-J. Shen,[b] Kenneth J. D. MacKenzie,[c] Ian W. M. Brown[c] and G. Vaughan White[c]

[a]*Department of Inorganic Chemistry, Arrhenius Laboratory, Stockholm University, S-106 91 Stockholm, Sweden*

[b]*Department of Materials Science & Engineering, Zhejiang University, Hangzhou 310 027, People's Republic of China*

[c]*New Zealand Institute for Industrial Research and Development, P.O. Box 31–310, Lower Hutt, New Zealand*

Simultaneous carboreduction and nitridation (CRN) of Y_2O_3 doped SiO_2/clay or elemental Si/clay mixes at atmospheric pressure were used to prepare low-cost powders of α-sialon composition. The synthesised products contained crystalline phase mixtures of α- and β-sialon and $Y_3Si_6N_{11}$. Subsequent hot pressing of the CRN powders at 1800 °C resulted in poorly densified materials from mixtures with low Y_2O_3, whereas high Y_2O_3 gave dense ceramics. The addition of SiO_2 to the starting mix resulted in ceramics containing substantial amounts of very fine SiC particles distributed in a matrix of β-sialon and glass. Solid state MAS NMR indicates that the crystalline SiC observed by XRD after hot-pressing is also present in an XRD-amorphous form in the pre-pressed powders, and that hot-pressing causes the Al—N units to become overall more oxygenated, with the conversion of β-sialon to α-sialon and the formation of small amounts of polytypoid sialons. The hardness, H_{V10}, and fracture toughness, K_{1C}, of the densified materials were *ca.* 18 GPa and 3 MPa $m^{1/2}$, respectively. The use of elemental Si produced less SiC, the major phase in these ceramics being α-sialon and a residual glassy phase observable by electron microscopy. The hardness and toughness of these densified materials was *ca.* 20 GPa and 3 MPa $m^{1/2}$, respectively.

Sialon ceramics exhibit good high temperature corrosion and mechanical properties.[1–3] Previous work, which has been mainly on β-sialon or α–β-sialon ceramics, has shown that these materials have good stability in oxidising and other corrosive atmospheres and in molten aluminium or copper alloys. These ceramics also have good thermal shock resistance, making them suitable for applications where rapid thermal changes occur. Both α–β-sialons with a high α-phase content and α-sialon ceramics are particularly suitable as high temperature materials, since the residual glassy phase can be reduced to a minimum.[4] This report focuses on the preparation of α-sialon ceramic compositions.

Typically, the preparation of sintered sialon ceramics involves the use of high purity silicon nitride and various additives. This gives a high cost product, which may not be necessary for all technical applications. Therefore attempts have been made to find alternative synthesis routes using low-cost starting materials. Previous work has shown that β-sialon ceramics can be prepared from clay minerals by simultaneous carbothermal reduction and nitridation (CRN).[5–11] The CRN processing of clays normally requires temperatures of 1400–1450 °C at atmospheric nitrogen pressure. The resulting powder is very fine grained and therefore highly reactive, which lowers the subsequent sintering temperatures and can lower the amount of additive necessary for full densification.

One drawback to clay precursors is the production of a CRN powder product with a high Al/Si ratio because of the high Al_2O_3/SiO_2 ratio of the clay itself. For example, the CRN process using New Zealand (NZ) halloysite clay results in β-sialon powder, $Si_{6-z}Al_zO_zN_{8-z}$, with $z = 2.3$–2.6.[10,12,13] The SiO_2 content of the clay must be increased by the addition of extra silica in order to produce a CRN powder which will sinter to low-z β-sialon ceramic.[14,15] In the present study, yttria (Y_2O_3) was also added in amounts which ensured that the overall compositions of the CRN products corresponded to Y-α-sialon ($Y_xSi_{12-4.5x}Al_{4.5x}O_{1.5x}N_{16-1.5x}$, where $x = 0.3$, 0.5 and 0.7). These powders were then used to prepare sintered sialon ceramics.

An alternative CRN reaction path, which gives similar α-sialon compositions from NZ halloysite clay, involves the substitution of silica by elemental silicon which has the ability to nitride in a controlled way, provided the temperature is kept well below the melting point of Si (*ca.* 1410 °C). The 'extra' driving force resulting from the exothermic nitridation of silicon allows the preparation of α-sialon powders from Si, clay and yttria mixes by an initial CRN process at lower temperatures. This reaction, and the sintering of the resulting α sialon powders, was also investigated in this work.

Experimental

Mixtures were made of halloysite clay, Y_2O_3, carbon and either SiO_2 or elemental Si to produce α-sialon powders with the overall composition $Y_xSi_{12-4.5x}Al_{4.5x}O_{1.5x}N_{16-1.5x}$ ($x = 0.3$, 0.5 and 0.7). The starting materials were New Zealand halloysite (NZ China Clays Ltd), carbon black (Degussa Lampblack), silicon dioxide (Silica Superfine, $D_{50} = 1.45$ μm, Commercial Minerals Ltd), elemental silicon (Sicomill, grade 4D, $D_{50} =$ 4.6 μm, KemaNord Industrikemi, Sweden) and yttrium oxide (Y_2O_3 Fine, grade C, H. C. Starck-Berlin). The halloysite was of good quality, with low impurity levels (Table 1), but contained 9% of residual crystalline silica which was taken into account when formulating the mixtures. The amount of carbon added corresponded to the calculated amount for complete CRN reaction plus a 10% excess.

The clay mixtures were blended with carbon by ball-milling in ethanol (4 h), dried in a rotary evaporator and extruded into 4 mm diameter rods. The samples were heated in alumina crucibles in a horizontal tube furnace (40 mm internal diameter). The firings were made in oxygen-free nitrogen gas (flow

Table 1 Major impurities of starting materials, taken from the supplier's specifications

atom%	clay	silicon	silica
Fe	0.18	0.08	0.02
Ca	trace	0.01	—
Mg	trace	—	—
Ti	0.03	—	0.006
Cr	—	—	0.0004

rate 100 ml min^{-1}); the mixtures containing silica were reacted at 1475 °C for 8 h, and those containing elemental silicon were pre-reacted at 1350 °C for 4 h then fired at 1475 °C for a further 8 h.

The reacted CRN products were compacted into pellets (*ca.* 5 g each) in a steel die and hot pressed in BN-coated graphite dies at 1800 °C (32 MPa pressure, holding time 2 h) in a graphite-resistance furnace under a protective nitrogen atmosphere.

The densities of the sintered specimens were measured using Archimedes principle. Before further physical characterisation, the pellets were carefully polished to 1 μm finish by standard diamond polishing techniques. Hardness (H_{v10}) and indentation fracture toughness (K_{1c}) at room temperature were measured using a Vickers diamond indenter with a 98 N (10 kg) load, and the fracture toughness was evaluated according to the method of Anstis *et al.*,[16] assuming a value of 300 GPa for Young's modulus.

The crystalline phases were determined by X-ray powder diffraction using a Guinier–Hägg focusing camera with Si as internal standard. The X-ray films were evaluated by a computer-linked scanner and the cell parameters determined by a least squares program. The *z*-value of β-sialon phase $Si_{6-z}Al_zO_zN_{8-z}$ was obtained both from the XRD unit cell dimensions according to the equations given by ref. 17 and directly by SEM-EDS analysis.

A scanning electron microscope (SEM, JEOL 880 equipped with Link AN 10000 energy-dispersive spectrometer, EDS) was used to investigate the microstructure of the fired pellets. Prior to the SEM investigations the samples were carefully polished and carbon-coated. Calibration curves were used to correct the EDS data, in which the estimated errors in the reported Y, Si, and Al contents of the sintered α-sialons were about *ca.* ±5%. Table 2 lists the overall starting compositions, together with those of the hot-pressed samples (in atom%) determined by EDS.

The CRN powders were also examined by ^{27}Al and ^{29}Si solid state magic angle spinning nuclear magnetic resonance, MAS NMR, at 11.7 T using a Varian Unity 500 spectrometer and 5 mm Doty high-speed probe spun at 10–12 kHz.[18] The ^{29}Si spectra were acquired using a 90° pulse of 6 μs and a recycle delay of 100 s, and were referenced to tetramethylsilane (TMS). The ^{27}Al spectra were acquired using a 15° pulse of 1 μs and a recycle delay of 1 s, and were referenced to $Al(H_2O)_6^{3+}$.

Table 2 Calculated overall starting compositions and compositions measured by EDS of hot-pressed samples. The intended compositions were designed to be on the α-sialon line $Y_xSi_{12-4.5x}Al_{4.5x}O_{1.5x}N_{16-1.5x}$

		starting overall (atom%)			EDS measured (atom%)		
sample		Si	Al	Y	Si	Al	Y
Si:	$x=0.3$	86.6	11.0	2.4	85.7	11.6	2.7
	$x=0.5$	78.0	18.0	4.0	78.4	17.4	4.2
	$x=0.7$	69.7	24.8	5.6	67.5	26.5	6.0
SiO_2:	$x=0.3$	86.6	11.0	2.4	88.0	9.5	2.5
	$x=0.5$	78.0	18.0	4.0	76.3	19.4	4.3
	$x=0.7$	69.7	24.8	5.6	67.4	27.6	5.0

Results and Discussion

Powder preparation by CRN

In a series of preliminary experiments we found that crystalline SiC, detectable by XRD, started to form around 1500 °C and became significant at temperatures above 1550 °C. However, α-sialon formation is also temperature dependent; it was therefore necessary to select an optimum temperature for the CRN process which also produced the minimum amount of SiC. The temperature of 1475 °C was chosen for the present CRN powder preparation.

The reacted CRN powders were homogeneous throughout the sample bulk, with a light-grey colour indicating the absence of residual carbon black. The XRD results showed that none of the starting materials was present. Table 3 summarises the crystalline phases present in the reacted rod-like powder granulates, which did not contain hard agglomerated particles and were easily crushed into fine powder.

XRD showed only slight differences in the crystalline phase compositions of reacted mixtures containing silica or elemental Si (Table 3). The XRD traces typically contained a weak, broad background hump indicating the presence of X-ray amorphous phases.The $Y_3Si_6N_{11}$ was identified on the basis of the XRD data of ref. 19, and its amount increased with increasing yttria content in the starting mix. The presence of this phase, together with crystalline β-sialon, suggests that not all the Y is used in α-sialon formation. The β-sialon had a *z*-value of *ca.* 0.4, indicating that the addition of elemental Si or silica to the CRN mixture has the desired effect of lowering the overall Al/Si ratio.

Since XRD sees only the crystalline products, possible amorphous phases (silica, SiC or other residual C-intermediates) are better investigated by MAS NMR, which has previously been used to demonstrate the presence of Si—C bonds in sialon powders prepared by CRN.[12,13] The reactions of halloysite clay with or without Y_2O_3 additions have been shown to be complex and temperature-dependent.[18] The clay initially forms mullite ($Al_6Si_2O_{13}$) and amorphous silica at intermediate temperatures. The silica is carbothermally reduced *via* a series of oxynitrides which become progressively more N-rich. SiC and Si_3N_4 are also formed, the latter reacting further with the mullite. β-sialon and Y-containing α-sialon form preferentially at higher temperatures and longer reaction times, but residual SiC was readily detected by MAS NMR in the fully reacted CRN products, even when not visible to XRD.

Some typical ^{29}Si and ^{27}Al MAS NMR spectra of the CRN powders are shown in Fig. 1.

The ^{29}Si spectra show resonances corresponding to SiC (δ *ca.* −16 to −18), the Si—N bonds in α-sialon, which coincide with the resonance[13] of α-silicon nitride and β-sialon (δ −47.5 to −48.5) and uncombined silica or silica-rich glass (δ −106 to −116). The relative intensities of these resonances reflect the composition of the various samples, and range from SiC-rich (in the samples derived from silica) to α-sialon-rich (in the samples derived from elemental Si). A small peak of variable intensity which occurs in some of the samples at δ −35 to −37 indicates the presence of $Y_3Si_6N_{11}$ in these

Table 3 Crystalline phase composition by XRD of the prepared CRN powders from NZ halloysite clay (1475 °C)

sample		observed phases
Si:	$x=0.3$	β-sialon ($z=0.55$),[a] $Y_3Si_6N_{11}$, α-sialon
	$x=0.5$	β-sialon ($z=0.38$), $Y_3Si_6N_{11}$, α-sialon
	$x=0.7$	β-sialon ($z=0.32$), $Y_3Si_6N_{11}$, α-sialon
SiO_2:	$x=0.3$	β-sialon ($z=0.31$), $Y_3Si_6N_{11}$, α-sialon
	$x=0.5$	β-sialon ($z=0.35$), $Y_3Si_6N_{11}$, α-sialon
	$x=0.7$	β-sialon ($z=0.35$), $Y_3Si_6N_{11}$, α-sialon

[a]Determined by XRD film.

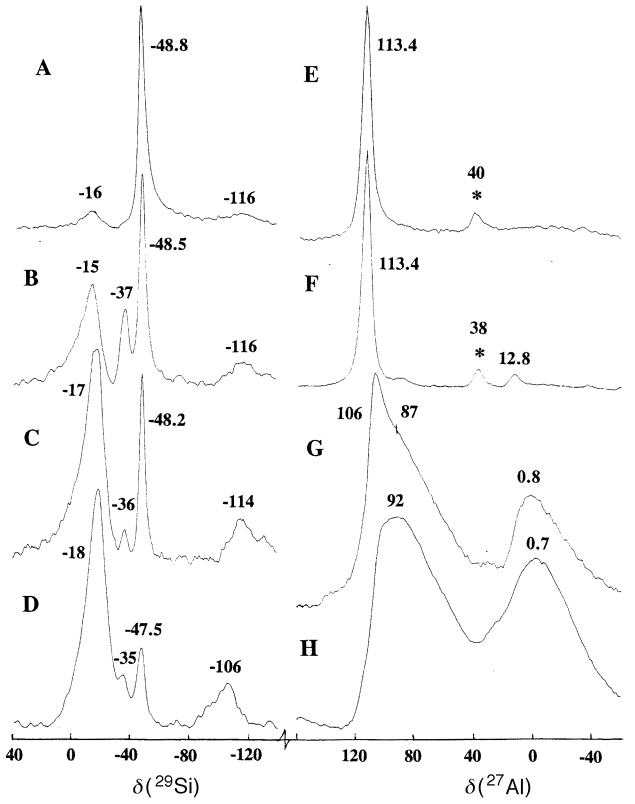

Fig. 1 Typical 11.7 T ^{29}Si and ^{27}Al MAS NMR spectra of α-sialon powders. A, Unpressed precursor derived from Si, $x=0.3$; B, unpressed precursor derived from Si, $x=0.7$; C, unpressed precursor derived from silica, $x=0.5$; D, unpressed precursor derived from silica, $x=0.7$; E, unpressed precursor derived from silica, $x=0.3$; F, unpressed precursor derived from Si, $x=0.7$; G, hot pressed sample derived from silica, $x=0.7$; H, hot pressed sample derived from Si, $x=0.5$. Asterisks denote spinning side bands.

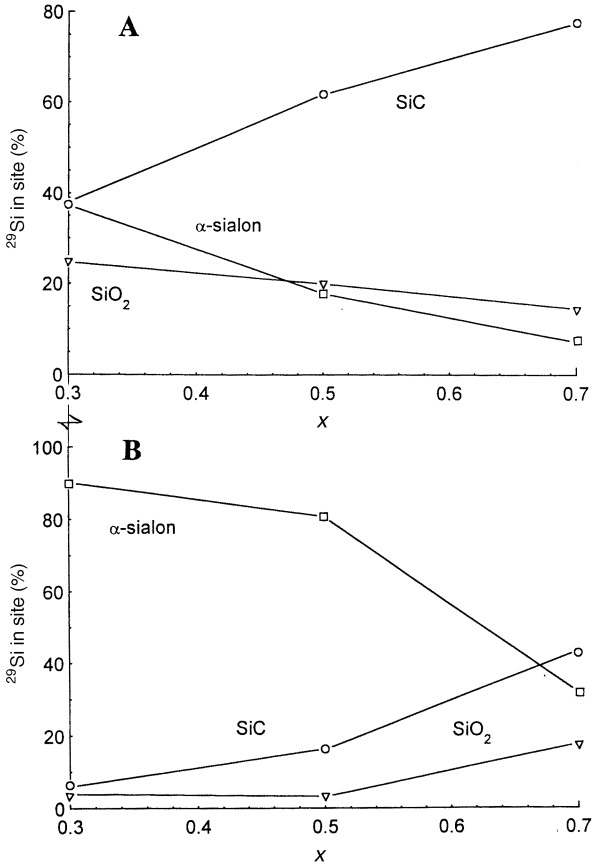

Fig. 2 Distribution of ^{29}Si over the various phases in unpressed α-sialon precursors as a function of composition x. A, derived from silica; B, derived from Si.

samples,[19] confirming the XRD identification of this phase in some of the samples. The distribution of ^{29}Si in the various phases in the CRN powders before hot pressing, estimated semi-quantitatively by curve-fitting the NMR spectra, is shown in Fig. 2. The technique does not distinguish between the α and β-sialon known from XRD to occur in the present samples.

As noted above, considerably more ^{29}Si is associated with SiC in the samples derived from silica-containing mixtures (Fig. 2A) than in Si-containing mixtures (Fig. 2B); however in samples derived from both silica and Si, the relative sialon content decreases and the SiC content increases with increasing x-values of the starting mixtures, as judged from the NMR distribution of ^{29}Si. Against the general trend, the glass content was slightly increased in the $x=0.7$ sample derived from Si.

The ^{27}Al MAS NMR spectra of all the samples prior to hot-pressing (Fig. 1E and F) are dominated by a sharp Al—N resonance at δ 113.4 corresponding to the structural units of α- and β-sialon. A previous study of carbothermal β-sialon formation[13] showed a predominance of the δ 113 resonance in highly-reacted samples containing significant proportions of β-sialon, and discussed possible reasons for the displacement of this resonance from the previously-reported position of δ 103–109.[20] The previous work[13] suggests the appearance of the major ^{27}Al resonance at δ 113 is not incompatible with the present semi-quantitative XRD observation of significant concentrations of β-sialon in these carbothermal precursors. The $x=0.7$ samples derived from both silica and Si (Fig. 1F) also showed a small resonance at δ *ca.* 91, assigned on the basis of Smith[21] and Fitzgerald *et al.*[22] to AlO_2N_2 units. The same samples also showed a small octahedral ^{27}Al resonance which is sometimes associated with β-sialon,[13] but may also contain a contribution from the substitution of a small amount of Al in the siliceous glass phase. The peak at δ 38–40 is a spinning side band from the major Al—N resonance. Thus, as the Al content increases, a small amount of the Al becomes associated with the more oxygenated regions of the body.

The CRN technique has also been used by others to prepare powders of α-sialon composition from mixtures of $CaSiO_3$, SiO_2 and Al_2O_3 with carbon black.[23] Heating at temperatures up to 1450 °C resulted in products containing mixtures of crystalline α- and β-sialon phases similar to our study. No other X-ray crystalline Ca-compound was observed. Re-firing these powders at $\geqslant$1500 °C or alternatively, carrying out the CRN reaction at these higher temperatures formed 95 mass% of α-sialon and SiC. The amount of SiC increased with temperature and became substantial at 1650 °C, as in our own preliminary observations of the CRN process (see above).

Hot-pressing

The sialon powders formed by CNR synthesis at 1475 °C were densified by hot pressing (HP) at 1800 °C for 2 h. Density measurements indicated that the CRN ceramics with the formulation equivalent to an α-sialon of $x=0.3$ (*i.e.* $Y_{0.3}Si_{10.65}Al_{1.35}O_{0.45}N_{15.55}$) were not fully dense. The available amorphous silica and/or the yttrium released by decomposition of the $Y_3Si_6N_{11}$ could not form sufficient low-viscosity liquid during sintering to allow full densification. In mixes where $x=0.5$, the sample containing the additional silica was dense, whereas the mix containing elemental Si did not form a fully dense ceramic. All the samples containing the highest Y-concentration ($x=0.7$) achieved high densities (Table 6).

The difference in sintering behaviour of the $x=0.5$ samples derived from SiO_2 and elemental Si can be understood by comparing the XRD crystalline phase composition of the

Table 4 Crystalline phase composition by XRD of the sintered ceramics after hot pressing of the CRN powders at 1800 °C for 2 h, *cf.* Table 3 and text

sample		observed phases
Si:	$x=0.3$	β-sialon ($z=0.45$),[a] α-sialon, (SiC)[b]
	$x=0.5$	α-sialon, (SiC),[b] [21R][c]
	$x=0.7$	α-sialon, SiC, (21R), [(M)]
SiO_2:	$x=0.3$	SiC, α-sialon, β-sialon ($z=0.28$),
	$x=0.5$	SiC, β-sialon ($z=0.35$), (α-sialon), [21R]
	$x=0.7$	SiC, (β-sialon), (12H)

[a]Determined by XRD film. 12H and 21R denotes the corresponding sialon polytypoid phases, M is melilite. [b]Parentheses indicate minor amounts by XRD. [c]Square brackets indicate trace amounts of a phase.

sintered samples (Table 4). The Si-derived samples contained mainly α-sialon which consumed most of the available Y, whereas the SiO_2-derived samples contained only small amounts of α-sialon, leaving most of the added Y available to take part in liquid formation at the pressing temperature (1800 °C).

XRD phase composition of sintered α-sialon ceramics

Table 4 summarises the crystalline phases detected by XRD in the various sintered materials. Different phase compositions were found in the sintered samples derived from elemental Si or SiO_2; the latter samples contain substantial amounts of crystalline SiC, with the $x=0.7$ material displaying XRD characteristics more typical of an SiC ceramic than one based on sialon (Table 4). By contrast, much more α-sialon was formed in sintered materials based on elemental Si.

The z-value of β-sialon, where formed, was always low, typical of a compound of composition close to β-Si_3N_4 with only small substitution of Al for Si. The β-sialon composition was very similar in the pre-reacted CRN powders and the sintered compacts (Tables 3 and 4), suggesting that high-temperature sintering had little effect on the residual β-sialon phase.

The hexagonal lattice parameters of the α-phases, calculated from the XRD data, indicate fairly similar compositions, (Table 5), the observed increase in the α-phase unit cell with increasing x-value (Y-content) being less than expected.[24] It is difficult to establish from these data the α-sialon composition in a two-dimensional phase field, but the EDS analysis gives a better estimate (see below). Small amounts of sialon polytypoid phases, occurring close to the AlN corner of the Si–Al–O–N phase diagram, were observed in all samples. The presence of the latter was confirmed by the microstructural study and the SEM-EDS analysis.

Although the XRD traces of the pre-reacted powders derived from the different starting mixes were very similar, the differences in XRD phase composition became much more apparent after high temperature sintering. This suggests that the differences between the pre-reacted powders were primarily in the X-ray amorphous phases, which became more XRD-visible during subsequent high-temperature sintering reactions. Thus, the pre-reacted powders based on elemental Si formed the desired α-sialon phase and smaller amounts of SiC and other phases. The substantial amounts of crystalline SiC formed at 1800 °C from silica-based precursor powders suggest the presence of significant numbers of Si—C bonds in the precursor. The small amount of SiC formed during sintering of the Si-derived precursors may result from the presence of the 9% silica in the original halloysite clay.

The ^{29}Si MAS NMR spectra of the hot-pressed samples show similar features to the spectra of the unpressed powders, but with only slight evidence of $Y_3Si_6N_{11}$ (δ 36). The semi-quantitative distribution of the ^{29}Si over the α-sialon, SiC and siliceous glassy phases is shown in Fig. 3.

Comparison of Fig. 3 with the corresponding data for the unpressed powders (Fig. 2) shows that the hot pressed samples retain similar ^{29}Si characteristics to the powders from which they were fabricated. The resonances of the small amounts of polytypoid sialon and melilite detected by XRD should appear at δ *ca.* −48[13] and −57[25] respectively but are apparently masked by the major sialon peak. Fig. 1G,H shows that hot pressing induces considerable changes in the ^{27}Al spectra, which are severely broadened and contain increased octahedral intensity centred at δ *ca.* 0.8, reflecting an increase in the concentration of sialon poytypoids, which typically contain AlO_6 resonances.[26] The broadening and shift of the original Al—N resonance at δ 113 to δ *ca.* 90–106 suggests the presence a continuum of Al—O—N units; the resonance maximum at δ 106 in the silica-derived samples (Fig. 1G) suggests a preponderance of $AlON_3$ units, with smaller numbers of AlO_2N_2 and AlO_3N units accounting for the shoulder at δ *ca.* 80–89.[21,22] The Si-derived samples (Fig. 1H) show the broad maximum at δ *ca.* 92, suggesting that the Al—N species are generally more oxygenated than in the analogous silica-derived samples. The reason for this, and the typically larger content of octahedral Al in these samples, is not immediately obvious.

Table 5 Analysis by XRD and EDS of the α- and β-sialon phases observed in hot-pressed samples, *cf.* text

		XRD					EDX				
		α		β			α			β	
sample		a/Å	c/Å	a/Å	c/Å	z	x	m	n	z	polytype Al/(Al+Si)
Si:	$x=0.3$	7.8120	5.6917	7.6173	2.9179	0.45	0.45	1.36	0.42	0.4	
	$x=0.5$	7.8154	5.6951	—	—	—	0.51	1.53	0.5	—	0.70
	$x=0.7$	7.8193	5.6982	—	—	—	0.53	1.58	0.41	—	0.72
SiO_2:	$x=0.3$	7.8123	5.6907	7.6125	2.9130	0.28	0.51	1.53	0.30	0.2	
	$x=0.5$	—	—	7.6150	2.9146	0.35	—	—	—	0.3	0.72
	$x=0.7$	—	—	—	—	—	—	—	—	—	0.71

Table 6 Observed densities and mechanical properties of hot-pressed materials

overall x-value	Si			SiO_2		
	D/g cm^{-3}	H_V/GPa	K_{1c}/MPa m$^{1/2}$	D/g cm^{-3}	H_V/GPa	K_{1c}/MPa m$^{1/2}$
0.3	2.74	—	—	2.77	—	—
0.5	3.07	14±0.8	4.2±0.4	3.35	19.2±0.1	3.0±0.4
0.7	3.39	19.9±0.1	3.0±0.4	3.35	17.6±0.3	3.0±0.4

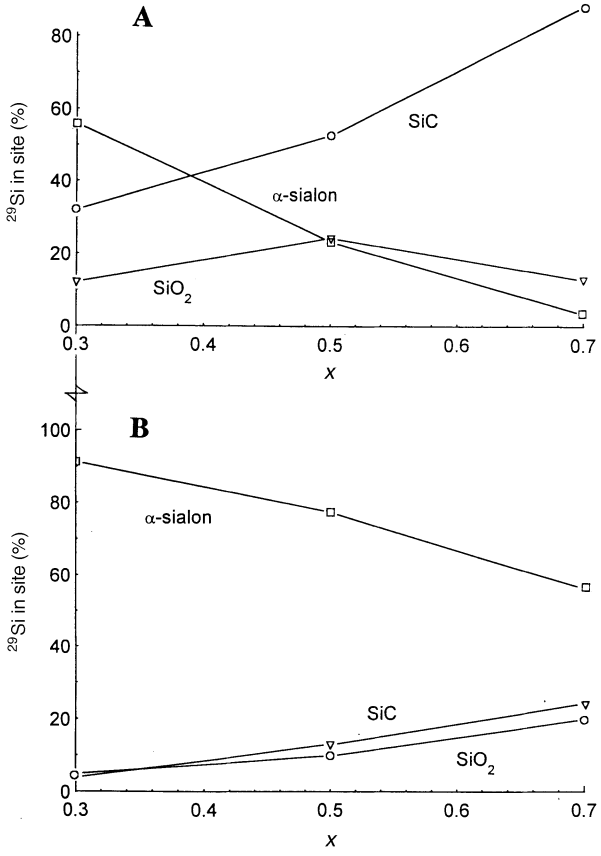

Fig. 3 Distribution of ^{29}Si over the various phases in hot-pressed α-sialon bodies as a function of composition x. A, Derived from silica; B, Derived from Si.

SEM microstructure of sintered ceramics

Since yttrium has a much higher atomic number than the other constituents of the compacts, the Y-containing phases appear light grey in the SEM microstructural investigations. Thus, the light coloured glassy intergranular phase is Y-rich, by contrast with the medium-grey α-sialon grains and the dark-coloured pores, β-sialon, SiC and sialon polytypoids. The latter phases can be distinguished from each other by their morphology or by their EDS elemental analysis.

All the microstructures were fine grained, with porosity evident in some. The mixtures of different phases of differing contrast resulted in micrographs of jumbled appearance, but with trends in the assembly of major phases broadly consistent with the XRD data of Table 4. The micrographs suggest that the amount of extremely fine-grained SiC and thin polytypoid crystals might be underestimated by XRD, which also does not detect the glassy phase shown by SEM to be present in all the microstructures, especially in materials with low α-sialon content.

The two samples of $x=0.3$ composition contained, in addition to the α- and β-sialon, considerable porosity and about 10 vol % of glass (the latter was difficult to estimate, however). Very fine dark spots (<0.1 μm) seen in the glassy phase of the SiO_2-derived material and occasionally in the Si-derived sample, are assumed to be nanosized SiC particles.

The microstructural features of ceramics synthesised with elemental Si ($x=0.5$ and 0.7) are shown in Fig. 4(*a*)–(*c*). The overall microstructure of the $x=0.5$ sample is dominated by medium-grey 0.5–2 μm α-sialon grains unevenly distributed in a glassy phase [Fig. 4(*a*)]. The sample also contains some fairly large pores and patterned glass areas containing small dark grains of polytypoid sialon. The Al/(Al+Si) ratio of 0.70, determined by EDS, suggests that these are not β-sialon, and the ratio is also a little low for the more AlN-rich polytypoids.

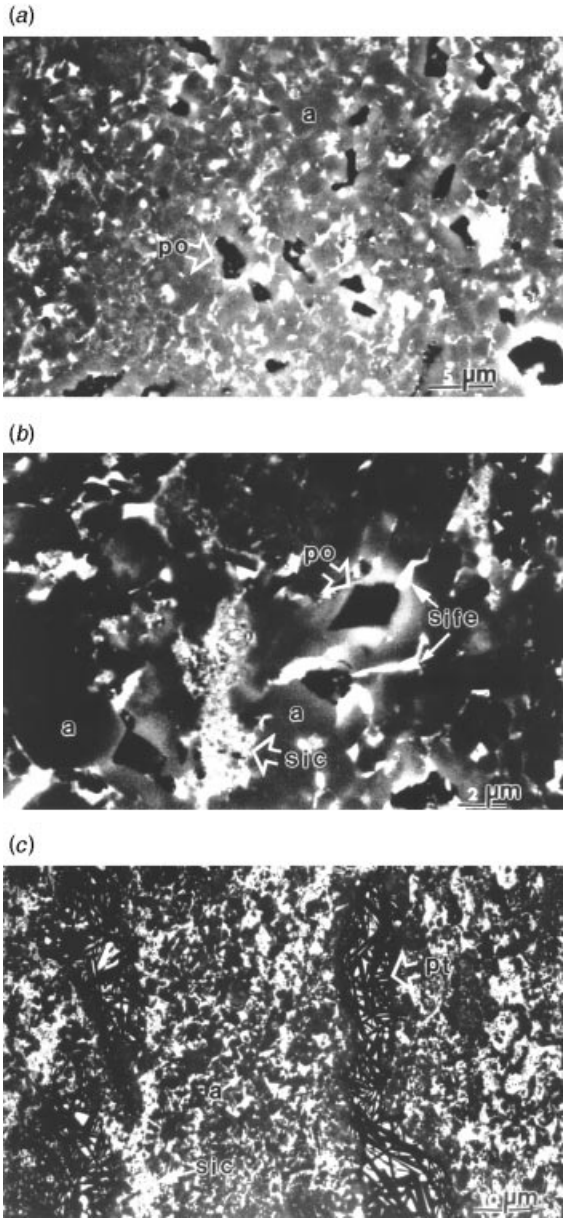

Fig. 4 SEM micrographs of sintered microstructures of samples with the composition $x=0.5$ prepared from CRN powders containing elemental Si. In (*a*) and (*b*) an overall impression of the microstructure and a detail showing nanosized SiC formation in a glassy pocket are illustrated, respectively. The microstructure at the composition $x=0.7$ is shown in (*c*). The α-sialon, porosity, nanosized SiC, iron silicides and sialon polytypoids are denoted by a, po, sic, sife, and pt, respectively.

One possible explanation for this Al/(Al+Si) ratio is the presence of Al–Si–C phases such as might be present in an environment high in SiC. The nanosized SiC occurs as agglomerates in some of the glassy pockets between the grains, [Fig. 4(*b*)]. The very bright 1–2 μm particles located in the grain boundaries are shown by EDS to contain high amounts of Fe and Si. The microstructure of the $x=0.7$ sample contained much more glassy phase, consistent with the decreased α-sialon content. The most striking features of this microstructure are the long agglomerates of polytypoid crystals formed in the unevenly distributed glassy phase [Fig. 4(*c*)].

The microstructural features of ceramics synthesised with SiO_2 ($x=0.5$ and 0.7) are illustrated in Fig. 5(*a*) and (*b*). A substantial amount of Y-containing glassy phase is seen, with the α-sialon either absent or present in only minor amounts. The $x=0.5$ sample contains some elongated β-sialon grains and large, uneven agglomerates of polytypoid crystals

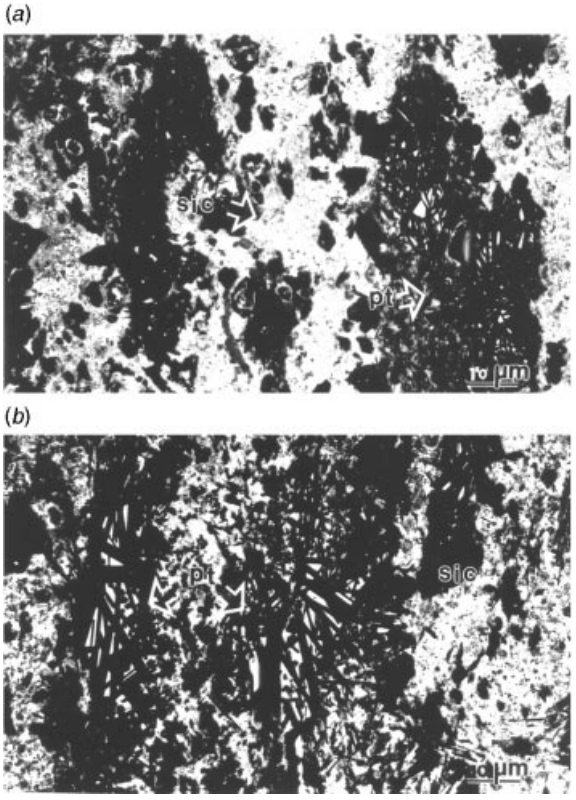

Fig. 5 SEM micrographs of sintered microstructures of samples prepared from CRN powders containing additional silica. In (*a*) and (*b*) the sample compositions $x=0.5$ and 0.7 are shown, respectively.

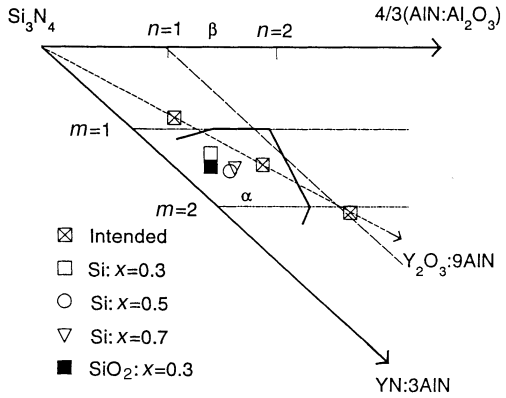

Fig. 6 Part of the Y–Si–Al–O–N phase diagram where the extension of the two-dimensional α-sialon solid solution (α′) is shown according to previous work.[24] The overall compositions of the present powders fall along the Si_3N_4–Y_2O_3·9AlN tie line and are indicated in the figure. All the α-phases formed by sintering at 1800 °C are of different composition from this mixture, falling within a fairly narrow compositional area.

[Fig. 5(*a*)]. The glassy phase forms a continuous matrix containing nanosized SiC grains (the small dark dots). A similar situation is found for the $x=0.7$ sample, but with increased amounts of polytypoid sialon and only occasional β-sialon and nano-sized SiC grains [Fig. 5(*b*)]. There is no microstructural evidence of α-sialon formation in this sample.

EDS analysis of the sialon polytypoid crystals indicated Al/(Al+Si) ratios of *ca.* 0.71, irrespective of their crystal morphology (Table 5), again suggesting that they are either of AlN-poor composition or contain Al–Si–C phases. The EDS analyses of the α-sialons are plotted on the plane of the Y–Si–Al–O–N system containing α-phase (Fig. 6), showing that all the present α-sialons fall in a small compositional area in the middle of the stability region, but shifted from the compositions of the starting mixtures.

Iron silicides, $FeSi_x$, were formed in the samples derived from elemental Si, but not in the SiO_2-derived samples. These phases result from the Fe impurity present in the Si powder (and clay) and their low melting points enable them to assume the shape of the surrounding grains at the sintering temperature.

The structures of the observed sialon polytypoid phases are based on the wurtzite structure of the parent AlN phase.[27] The sialon polytypoids have extended solid solution ranges along lines with constant metal/non-metal ratio $(Si,Al)_x(O,N)_{x+1}$ where $4\leqslant x\leqslant 9$ and are conveniently described by Ramsdell terminology in which the 12H and 21R phases observed here correspond to $x=6$ and 7, respectively. Thus, they are closely similar in terms of both their metal/non-metal ratio and Si content. These compositions probably represent the high-Si end of the 12H and 21R solid solution ranges.

The formation of extremely fine grained (nanosized) SiC particles by sintering of CRN powders has previously been reported in $Y_{0.25}Si_{5.5}Al_{0.5}O_{0.5}N_{7.5}$ powder sintered at 1650–1720 °C;[11] this is not an α-sialon composition, but is very close to β-sialon with $z=0.5$ ($Si_{5.5}Al_{0.5}O_{0.5}N_{7.5}$) containing additional yttrium. The densified materials showed only the presence of β-sialon by XRD, but a careful electron microscopic examination of the microstructure revealed a complicated material consisting of equi-axed β-sialon grains (*ca.* 1 μm) bonded with a glassy phase containing occasional α-sialon grains < 0.5 μm in size. However, the most interesting feature was fine SiC grains (10–50 nm) which were found both as inclusions in β-sialon grains and in the glassy phase. The carbon source for this SiC is believed to be the 1.4% residual carbon in the pre-reacted CRN powder.

Mechanical properties

The measured Vickers hardness and indentation fracture toughness values are summarised in Table 6. These measurements were not made on the $x=0.3$ samples because of their poor densification (< 3.0 g cm^{-3}). The Si-derived sample with $x=0.5$ (*ca.* 90% theoretical density) shows anomalous results (low hardness but a fracture toughness greater than those of the fully dense materials). The fully dense materials are somewhat brittle and fairly hard, their properties being similar to those of glass-free polycrystalline α- or β-sialon ceramics.[2]

The mechanical properties of the present samples are surprisingly good, taking into account the presence of substantial amounts of glassy phase, which is of very low hardness (*ca.* 10 GPa) and is very brittle (~1 MPa m$^{1/2}$). It is possible that the presence of the nanosized SiC particles has a positive effect on the hardness and toughness of the glassy phase; silicon carbide is very hard and will increase the measured hardness, while small amounts of carbon might also alloy into the Y–Si–Al–O–N glass, increasing its hardness. It is known from other ceramic 'nanocomposites' that the toughness can be positively influenced in some cases by the presence of nanosized particles,[28,29] although the presence of SiC particles in monolithic Si_3N_4 is reported to produce no significant increase in its toughness (*ca.* 2.6 MPa m$^{1/2}$ with and without SiC particles).[30]

Conclusions

The CRN technique offers a method for obtaining low-cost sialon precursor powders. Adjusting the silicon content of the mixture by the addition of elemental Si instead of the more usual SiO_2 enhances the nitridation reactions at lower temperatures and forms less amorphous SiC. These pre-reacted powders are not easily densified, because most of the yttria added initially is consumed by the formation of nitrogen-rich

Y compounds (α-sialon and $Y_3Si_6N_{11}$), reducing the amount of available low-temperature low-viscosity eutectic liquids. High Y_2O_3 contents in the starting mix give dense ceramics.

The use of SiO_2 to adjust the composition of the starting mix produces ceramics containing substantial amounts of very fine SiC particles distributed in a matrix of β-sialon and glass. The use of elemental Si in the initial mix produces considerably less SiC and more α sialon, but a residual glassy phase is observed in the microstructure. The hardness, H_{V10}, and fracture toughness, K_{1C}, of the fully dense materials is *ca.* 18–20 GPa and 3 MPa $m^{1/2}$, respectively.

T. E. is grateful for an IRL Senior Research Fellowship which enabled him to participate in this study.

References

1 K. H. Jack, *J. Mater. Sci*., 1976, **11**, 1135.
2 T. Ekström and M. Nygren, *J. Am. Ceram. Soc*., 1992, **75**, 259.
3 T. Ekström, *Mater. Forum*, 1993, **17**, 67.
4 T. Ekström, *Proc. Austceram 90*, ed. P. J. Darragh and R. J. Stead, Trans Tech. Publ. Ltd, Perth, Australia, 1990, p. 586.
5 H. Mostaghaci, F. L. Riley and J. P. Torre, *Int. J. High Technol. Ceram*., 1988, **4**, 512.
6 S. Bandyopadhyay and J. Mukerji, *Adv. Ceram. Mater*., 1988, **3**, 328.
7 I. W. M. Brown, R. Pompe and R. Carlsson, *J. Eur. Ceram. Soc*., 1990, **6**, 191.
8 Y. W. Cho and J. A. Charles, *Mater. Sci. Technol*., 1991, **7**, 399.
9 E. Kokmeijer, G. de With and R. Metselaar, *J. Eur. Ceram. Soc*., 1991, **8**, 71.
10 I. W. M. Brown, *Proc. Austceram 92*, ed. J. Bannister, CSIRO, Melbourne, 1992, p. 494.
11 W.-C. J. Wei and J. W. Halloran, *J. Eur. Ceram. Soc*., 1994, **14**, 419.
12 M. E. Bowden, K. J. D. MacKenzie and J. H. Johnston, *Mater. Sci. Forum*, 1988, **34–36**, 599.
13 K. J. D. MacKenzie, R. H. Meinhold, G. V. White, C. M. Sheppard and B. L. Sherriff, *J. Mater. Sci*., 1994, **29**, 2611.
14 G. V. White, T. Ekström, I. W. M. Brown, G. C. Barris and C. M. Sheppard, *Proc. Austceram 96*, in press.
15 T. Ekström, G. V. White, I. W. M. Brown, G. C. Barris and C. M. Sheppard, *Proc. Austceram 96*, in press.
16 G. R. Anstis, P. Chantikul, B. R. Lawn and D. P. Marshall, *J. Am. Ceram. Soc*., 1981, **64**, 533.
17 T. Ekström and P.-O. Olsson, *J Am. Ceram. Soc*., 1989, **72**, 1722.
18 K. J. D. MacKenzie, T. Ekström, G. V. White and J. S. Hartman, *J. Mater. Chem*., 1997, **7**, 1057.
19 T. Ekström, K. J. D. MacKenzie, M. J. Ryan, I. W. M. Brown and G. V. White, *J. Mater. Chem*., 1997, **7**, 505.
20 R. Dupree, M. H. Lewis and M. E. Smith. *J. Appl. Crystallogr*., 1986, **21**, 109.
21 M. E. Smith, *J. Phys. Chem. Soc*., 1992, **96**, 1444.
22 J. J. Fitzgerald, S. D. Kohl, G. Piedra, S. F. Dec and G. E. Maciel, *Chem. Mater*., 1994, **6**, 1915.
23 J. W. T. van Rutten, R. A. Terpstra, J. C. T. van der Heijde, H. T. Hintzen and R. Metselaar, *J. Eur. Ceram. Soc*., 1995, **15**, 599.
24 Z.-J. Shen, L.-O. Nordberg, M. Nygren and T. Ekström, in *Engineering Ceramics '96: Higher Reliability Through Processing*, ed. G. N. Babini, M. Haviar and P. Sajgalik, Kluwer Academic, Dordrecht, 1997, p. 169.
25 R. H. Meinhold and K. J. D. MacKenzine, *Solid State Nucl. Magn. Reson*., 1995, **5**, 151.
26 N. D. Butler, R. Dupree and M. H. Lewis. *J. Mater. Sci. Lett*., 1984, **3**, 469.
27 D. P. Thompson, P. Korgul and A. Hendry, in *Progress of Nitrogen Ceramics*, ed. F. L. Riley, Nijhoff, The Hague, The Netherlands, p. 61.
28 K. Niihara, *J. Ceram. Soc. Jpn*., 1991, **99**, 974.
29 Y. Akimune, N. Hirosaki and T. Ogasawara, *J. Mater. Sci. Lett*., 1991, **10**, 223.
30 G. Pezzotti and M. Sakai, *J. Am. Ceram. Soc*., 1994, **77**, 3039.

Paper 7/07729G; *Received* 27*th October*, 1997